



### Atom Probe Analyses and Numerical Calculation of Ternary Phase Diagram in Ni-Al-V System

H. Zapolsky\*, C. Pareige, L. Marteau, D. Blavette

UMR 6634 CNRS Faculte des Sciences de Rouen, Universite de Rouen 76821 Mont Saint Aignan Cedex, France

L.Q. Chen

Department of Materials Science and Engineering, Penn State University, University Park, PA16802, USA

\*Corresponding author's email: zapolsky@scapin.univ-rouen.fr

**Abstract.** The ternary phase diagram in the Ni-Al-V system is studied using three dimensional atom probe (3DAP) analyses and numerical calculations using a mean-field model. Our focus is on the Ni-rich corner of the isothermal section at 800°C of the ternary phase diagram, where disordered f.c.c. matrix coexists with the L<sub>12</sub> and DO<sub>22</sub> ordered phases. Both the experimental measurements and numerical calculations showed that the equilibrium compositions of the coexisting phases are quite different from those predicted by published phase diagrams. It is demonstrated that the aluminium and vanadium compositions in the L<sub>12</sub> phase are approximately the same, and there is more aluminium in the disordered matrix than that indicated in the existing phase diagram. A possible explanation of this disagreement is discussed.

#### Introduction

The understanding of thermodynamics and phase diagrams in multicomponent systems is fundamental and essential in materials science. The knowledge of the equilibrium state at a given temperature is the starting point in the description of any phenomena or process.

This work is part of a more extensive project aiming at studying the transformation paths in NiAlV system by atom probe analyses and numerical simulations. As shown previously [1,2], the Ni-Al-V ternary phase diagram (fig.1) contains a three phase region at 800°C in which the disordered phase  $\gamma$  (fig. 2a) coexists with two ordered phases, namely  $\gamma'$  (Ni<sub>3</sub>Al, fig. 2b) which has an L<sub>12</sub> structure and  $\theta$  (Ni<sub>3</sub>V, fig. 2c) with the DO<sub>22</sub> structure.

The kinetics of  $\gamma \rightarrow \gamma' + \theta$  transformation was investigated by Chen et al. [3] and Bendersky et al [4]. However, they focused only on the pseudo-binary section of the phase diagram. We are systematically investigating the kinetics of compositional clustering and ordering in the ternary NiAlV system using the three dimensional atom probe (3DAP), microscopic mean field approaches, and Monte Carlo simulations [5]. In this paper we focus on the thermodynamics, namely, the equilibrium states in the three-phase region.

Isothermal cross sections of the phase diagram in Ni-Al-V were previously reported both experimentally and theoretically [1,2,5]. However, some discrepancies on the solubility limits of phases were shown recently to exist using 3DAP. One of the goals of this work is to understand the discrepancies and to validate a set of potentials which will be used in our kinetics modeling.

A mean field approach is used to calculate the equilibrium concentrations of the three coexisted phases at a given temperature. Ising Hamiltonian is written in terms of the amplitudes of static concentration waves related to both L<sub>12</sub> and DO<sub>22</sub> ordered structures as proposed by Khachatryan [6]. Effective pair interactions used by Chen in a previous work [3] are used. The numerical results are compared to atom probe data and published diagrams.

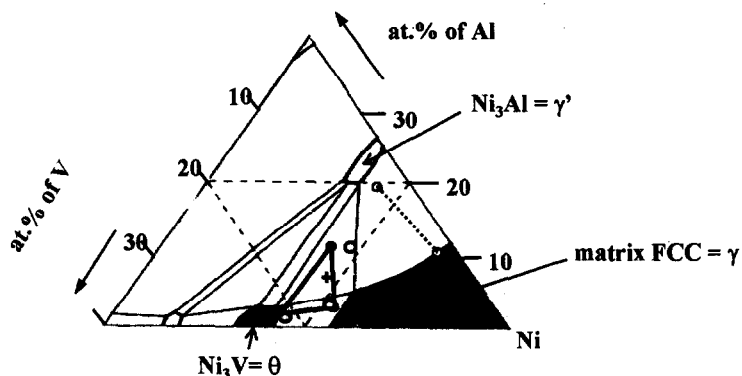


FIG.1

Isothermal section at 800°C of the ternary NiAlV phase diagram [2]. The cross corresponds to the composition of the alloy investigated by 3DAP (Ni-7at.% Al-14.5at.%V).

- correspond to the solubility limits measured by Jia *et al* [13].
- correspond to the solubility limits measured by 3DAP in the three phase alloy and
- correspond to the calculated solubility limits.

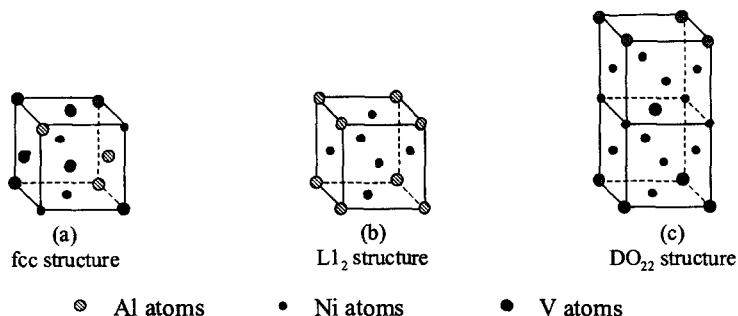


FIG.2

The crystal structure of the 2a - disordered matrix, 2b- L<sub>12</sub> superstructure and 2c- DO<sub>22</sub> superstructure.

### Experimental results

The 3DAP, developed at the University of Rouen, France, provides three-dimensional maps of chemical heterogeneities in a metallic material on a subnanometric scale [7-9]. 3DAP is based on the field evaporation of atoms from the specimen surface. The high electric field required to evaporate atoms from the surface is obtained by applying a high positive voltage ( $V_0 \approx 10\text{kV}$ ) to a sample prepared in form of a very sharp tip (curvature radius  $\approx 50\text{ nm}$ ). In order to generate reliable composition data, the tip is maintained at 40K. The sample is placed under high vacuum conditions ( $10^{-7}\text{ Pa}$ ). Surface atoms are evaporated by electric pulses ( $\approx 19\%$  of  $V_0$ ) superimposed on  $V_0$ . Then, the nature of the ions evaporated from the tip surface is known by time-of-flight mass spectrometry. A multi-impact spatial detector is used to determine the co-ordinates of ion impacts. The initial position of ions at the specimen surface is derived from a simple point projection law. The field evaporation of successive atomic layers in continuous way allows to reconstruct the analysed volume. The overall lateral spatial resolution at the sample surface is close to 0.3 nm whereas the depth resolution makes it possible to image low index planes.

We applied this technique to measure the equilibrium compositions of the L<sub>12</sub>, DO<sub>22</sub> and disordered f.c.c. phases in the NiAlV ternary system. Specimens with 7at.% of Al and 14.5at.% of V were prepared from <001> oriented single crystals at the ONERA (Office National d'Etudes et de Recherches Aérospatiales). After

homogenisation at 1300°C for 3h and quench into iced-brine, the samples were heat-treated at 800°C for 1h and 24 h. These treatments were immediately followed by a water quench.

By an appropriate choice of the analysis site, it is possible to image the chemical order in  $L_{12}$  precipitates and in two of the three orientation variants of the  $DO_{22}$  precipitates. The chemical order is revealed either by the basic stacking sequence of Al-rich (or V-rich) and Al-depleted (or V-depleted) (001) planes in the  $\gamma'$  (or  $\theta$ ) phase or by the presence of (024) V planes in  $\theta$  precipitates. Figures 3a and 3b show the three-dimensional distribution of vanadium and aluminium atoms, respectively. For clarity, only a small slice ( $15 \times 15 \times 50 \text{ nm}^3$ ) of the analysed volume is represented. The visualisation of chemical order and the measurements of local composition make it possible to clearly distinguish the different phases.

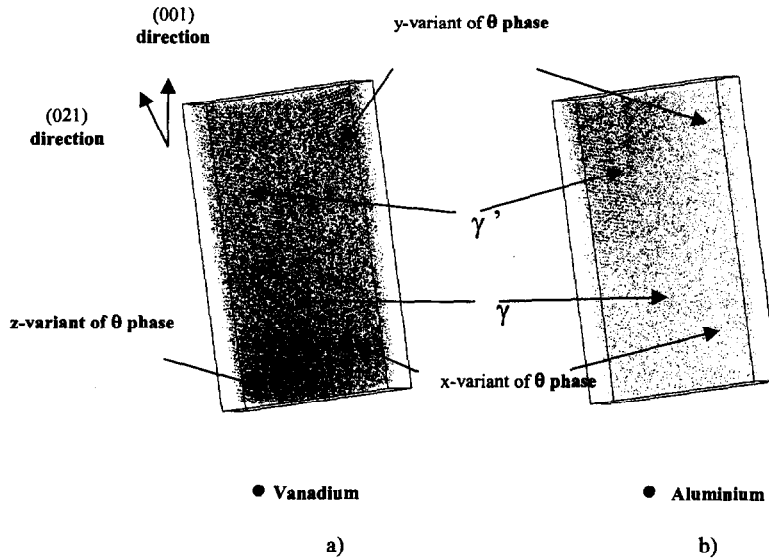


FIG.3

Three-dimensional Al (a) and vanadium (b) maps for Ni-7.5%Al-14.5%V single crystal aged for 1h at 800°C ( $V=15 \times 15 \times 50 \text{ nm}^3$ ). Each dot represents one vanadium or aluminium atom, respectively.

A composition depth profile that was derived from figure 3 is shown in figure 4. The  $\theta$  phase contains the highest concentration of vanadium while the  $\gamma'$  phase has the highest Al concentration. The compositions of  $\theta$ ,  $\gamma'$  and  $\gamma$  measured by 3DAP are given in table 1. We found no significant differences in the results obtained from the samples aged for 1h and for 24h at 800°C. Therefore, we are quite confident that these values correspond to the equilibrium ones. They are compared, table 1, to the compositions deduced from the existing NiAlV phase diagram. Within uncertainties, the composition we obtained for the  $DO_{22}$  is in good agreement with the existing phase diagram. The measured compositions of phase are also close to those determined from the existing phase diagram. However, the compositions of the  $L_{12}$  phase are quite different from the phase diagram. We found higher concentration of vanadium in the  $L_{12}$  phase than that described by the phase diagram. In spite of some possible artifacts inherent to the technique [9], the measured values strongly suggest that the NiAlV isothermal section at 800°C for the existing phase diagram needs to be modified.

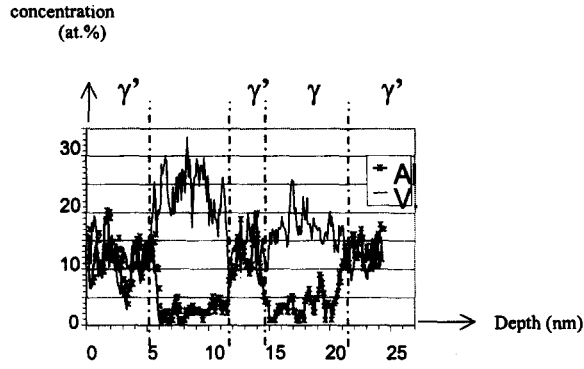


FIG.4

The aluminum, vanadium and nickel concentration profiles through the interfaces of the disordered f.c.c. phase and  $L_{12}$  and  $DO_{22}$  ordered phases.

TABLE 1

Equilibrium compositions of the  $\gamma$ ,  $\gamma'$  and  $\theta$  phases from 3DAP, numerical calculations using the mean-field model, and from a previously published ternary phase diagram.

		$\gamma$	$\gamma'$	$\theta$
3DAP (at.%)	Ni	$81.1 \pm 1.5$	$76.7 \pm 0.3$	$76.9 \pm 0.2$
	Al	$2.7 \pm 0.6$	$11.3 \pm 0.3$	$1.70 \pm 0.03$
	V	$16.2 \pm 1.4$	$12.0 \pm 0.3$	$21.4 \pm 0.2$
Phase diagram[2] (at.%)	Ni	82.4	74.8	75.5
	Al	4.8	19.7	2.7
	V	12.8	5.5	21.8
Simulations (at.%)	Ni	80.5	79.0	76.9
	Al	3.0	11.0	1.0
	V	16.5	10.0	21.1

### Microscopic Mean-Field Model

To evaluate the equilibrium composition of coexistent phases, we need the total Helmholtz free energy of each one. In the mean field model with the single site approximation, the free energy  $F$  for the ternary system is given by [3]:

$$\begin{aligned}
 F = & -\frac{1}{2} \sum_r \sum_{r'} [V_{AB}(\bar{r} - \bar{r}') P_A(\bar{r}) P_B(\bar{r}') + V_{AC}(\bar{r} - \bar{r}') P_A(\bar{r}) P_C(\bar{r}') + \\
 & V_{BC}(\bar{r} - \bar{r}') P_B(\bar{r}) P_C(\bar{r}')] + k_B T \sum_r [P_A(\bar{r}) \ln(P_A(\bar{r})) + P_B(\bar{r}) \ln(P_B(\bar{r})) + \\
 & (1 - P_A(\bar{r}) - P_B(\bar{r})) \ln(1 - P_A(\bar{r}) - P_B(\bar{r}))] \quad (1)
 \end{aligned}$$

where  $k_B$  is the Boltzmann constant,  $T$  is the temperature, the distribution functions  $P_A(\mathbf{r})$  and  $P_B(\mathbf{r}')$  represent the probabilities of finding an A and B atom at given lattice site  $\mathbf{r}$  or  $\mathbf{r}'$ , respectively, and

$$\begin{aligned}
 V_{AB}(\bar{r} - \bar{r}') &= W_{AA}(\bar{r} - \bar{r}') + W_{BB}(\bar{r} - \bar{r}') - 2W_{AB}(\bar{r} - \bar{r}') \\
 V_{BC}(\bar{r} - \bar{r}') &= W_{BB}(\bar{r} - \bar{r}') + W_{CC}(\bar{r} - \bar{r}') - 2W_{BC}(\bar{r} - \bar{r}')
 \end{aligned}$$

$$V_{AB}(\bar{r} - \bar{r}') = W_{AA}(\bar{r} - \bar{r}') + W_{BB}(\bar{r} - \bar{r}') - 2W_{AB}(\bar{r} - \bar{r}')$$

in which  $W_{\alpha\beta}(\mathbf{r}-\mathbf{r}')$  are the pairwise interaction energies between a pair of atoms,  $\alpha$  and  $\beta$  ( $=A, B$  or  $C$ ), at lattice site  $\mathbf{r}$  and  $\mathbf{r}'$ .

We can describe the atomic distribution in the ternary compound by only two distribution functions since the occupation probabilities  $P_A(\mathbf{r})$ ,  $P_B(\mathbf{r})$  and  $P_C(\mathbf{r})$  for A, B and C atoms, respectively, are not independent. They must satisfy the identity:

$$P_A(\bar{r}) + P_B(\bar{r}) + P_C(\bar{r}) = 1$$

To determine the distribution functions  $P_A(\mathbf{r})$  and  $P_B(\mathbf{r})$  and describe disorder-order transitions, we use the concentration waves approach firstly proposed by Khachaturyan [6]. In this approach the distribution function can be represented as a superposition of static concentration waves:

$$P(\bar{r}) = c + \frac{1}{2} \sum_s \eta_s \sum_{j_s} [(\gamma_s(j_s) \exp(i\bar{k}_{j_s} \cdot \bar{r}) + \gamma_s^*(j_s) \exp(-i\bar{k}_{j_s} \cdot \bar{r}))] \quad (3)$$

where  $c$  is the composition,  $\exp(i\mathbf{k}_{j_s} \cdot \mathbf{r})$  is a static concentration wave with the wave vectors  $\mathbf{k}_{j_s}$  which describe the ordered superstructure (index  $j_s$  denote the wave vectors in the first Brillouin zone of the star,  $s$ ),  $\eta_s$  is a long range order parameter which is equal to zero in a disordered state and unity in a fully ordered state, and  $\gamma_s(j_s)$  are coefficients that determine the symmetry of the occupation probabilities  $P(\mathbf{r})$  (the symmetry of the superstructure). The summation in eq. (3) is carried out over all vectors,  $\{j_s\}$ , of the star,  $s$ . In general case, the star  $\{k_s\}$  contains several wave vectors  $k_{1s}, k_{2s}, \dots, k_{ns}$ . All these vectors can be obtained from one vector (for example,  $k_{1s}$ ) by all the symmetry operations in the point-symmetry group of the disordered solution lattice.

The  $L1_2$  ordered structure is shown in fig.2b. This structure is generated by wave vector

$$k_1 = (k_x, k_y, k_z) = (2\pi h a_1^{-1}, 2\pi k a_2^{-1}, 2\pi l a_3^{-1}) \quad (4)$$

with  $a_1, a_2$  and  $a_3$  being the unit reciprocal lattice vectors of the f.c.c. lattice along [100],[010] and [001] directions, respectively, and  $|a_1| = |a_2| = |a_3| = 1/a_0$  ( $a_0$  is the lattice parameter of the f.c.c. lattice and  $h, k$ , and  $l$  are integers).

Using the static concentration wave method the distribution functions  $P_A(\mathbf{r})$  and  $P_B(\mathbf{r})$ , for an  $L1_2$  ordered structure, can be written:

$$\begin{aligned} P_A(\bar{r}) &= c_A(1 + \eta_{1A}(e^{2\pi i x} + e^{2\pi i y} + e^{2\pi i z})) \\ P_B(\bar{r}) &= c_B(1 + \eta_{1B}(e^{2\pi i x} + e^{2\pi i y} + e^{2\pi i z})) \end{aligned} \quad (5)$$

where  $c_A$  and  $c_B$  are the average composition of A and B in the ternary Ni-Al-V compound,  $\eta_{1A}$  and  $\eta_{1B}$  are the long-range order parameters for two type of the atoms,  $x, y$  and  $z$  are the f.c.c. lattice site coordinates (integers or half-integers). The distribution (5) assumes only two value  $c+3c\eta_1$  and  $c-c\eta_1$  on all lattice sites. Substituting eq.(5) into the general free energy expression eq.(1) yields immediately the free energy of the  $L1_2$  ordered phase per atom:

$$\begin{aligned} F(L1_2) &= \frac{1}{2} [(V_{BC}(\bar{0}) + V_{AC}(\bar{0}) - V_{AB}(\bar{0}))c_A c_B + V_{BC}(\bar{0})c_B^2 + V_{AC}(\bar{0})c_A^2] + \left(\frac{3}{2}\right) [\eta_{1A}^2 c_A^2 V_{AC}(\bar{k}_1) \\ &+ \eta_{1B}^2 c_B^2 V_{BC}(\bar{k}_1) + \eta_{1A} \eta_{1B} c_A c_B (V_{BC}(\bar{k}_1) + V_{AC}(\bar{k}_1) - V_{AB}(\bar{k}_1))] + \\ &\left(\frac{k_B T}{4}\right) [c_A(1 + 3\eta_{1A}) \ln(c_A(1 + 3\eta_{1A})) + c_B(1 + 3\eta_{1B}) \ln(c_B(1 + 3\eta_{1B})) + (1 - c_A(1 + 3\eta_{1A}) - c_B(1 + 3\eta_{1B})) \\ &\ln(1 - c_A(1 + 3\eta_{1A}) - c_B(1 + 3\eta_{1B}))] + \frac{3k_B T}{4} [c_A(1 - \eta_{1A}) \ln(c_A(1 - \eta_{1A})) + c_B(1 - \eta_{1B}) \ln(c_B(1 - \eta_{1B})) + \\ &(1 - c_A(1 - \eta_{1A}) - c_B(1 - \eta_{1B})) \ln(1 - c_A(1 - \eta_{1A}) - c_B(1 - \eta_{1B}))] \end{aligned} \quad (6)$$

where  $V_{\alpha\beta}(0)$  and  $V_{\alpha\beta}(\mathbf{k}_1)$  are the values of the Fourier transform of  $V_{\alpha\beta}(\mathbf{r})$  at  $\mathbf{k} = 0$  and  $\mathbf{k} = \mathbf{k}_1$ . In general case the Fourier transform of interatomic pairwise energy  $W(\mathbf{r})$  is

$$V(\vec{k}) = \sum_{\vec{r}} W(\vec{r}) e^{i\vec{k}\vec{r}}$$

Using a fourth nearest-neighbor interatomic model, for an f.c.c. lattice in the disordered phase  $V_{\alpha\beta}(\mathbf{0})$  is given by

$$V_{\alpha\beta}(\vec{0}) = 12 V_{\alpha\beta}^1 + 6 V_{\alpha\beta}^2 + 8 V_{\alpha\beta}^3 + 24 V_{\alpha\beta}^4 \quad (7)$$

In the case of an ordered  $L_{12}$  phase the  $V_{\alpha\beta}(\mathbf{k}_1)$  can be written as

$$V_{\alpha\beta}(\vec{k}_1) = -4 V_{\alpha\beta}^1 + 6 V_{\alpha\beta}^2 - 8 V_{\alpha\beta}^3 + 12 V_{\alpha\beta}^4 \quad (8)$$

In eq.(7) and (8)  $V_{\alpha\beta}^1$ ,  $V_{\alpha\beta}^2$ ,  $V_{\alpha\beta}^3$  and  $V_{\alpha\beta}^4$  are the first, second, third and forth-nearest neighbor effective interchange interaction parameters between  $\alpha$  and  $\beta$  atoms, respectively.

The  $DO_{22}$  ordered structure is shown in fig.2c. This structure is generated by two wave vectors

$$\begin{aligned} \vec{k}_2 &= 2\vec{k}_3 = 2\pi(2a_1^* + a_3^*) \\ \vec{k}_3 &= \pi(2a_1^* + a_3^*) \end{aligned} \quad (9)$$

The distribution functions for  $DO_{22}$  ordered phases can be written in the form

$$\begin{aligned} P_A(\vec{r}) &= c_A(1 + \eta_{2A} e^{2\pi i(2x+z)} + 2\eta_{3A} \cos \pi(2x+z)) \\ P_B(\vec{r}) &= c_B(1 + \eta_{2B} e^{2\pi i(2x+z)} + 2\eta_{3B} \cos \pi(2x+z)) \end{aligned} \quad (10)$$

where  $\eta_{2A}$ ,  $\eta_{2B}$ ,  $\eta_{3A}$  and  $\eta_{3B}$  are the long-range order parameters related to wave vectors  $\mathbf{k}_2$  and  $\mathbf{k}_3$ . These distribution functions take three values,  $c+c\eta_2+2c\eta_3$ ,  $c+c\eta_2-2c\eta_3$  and  $c-c\eta_2$ . Substituting eq. (10) into eq.(1) gives the free energy of the  $DO_{22}$  ordered phase

$$\begin{aligned} F(DO_{22}) &= \frac{1}{2} [(V_{BC}(\vec{0}) + V_{AC}(\vec{0}) - V_{AB}(\vec{0}))c_A c_B + V_{BC}(\vec{0})c_B^2 + V_{AC}(\vec{0})c_A^2] + \frac{1}{2}(c_A^2 \eta_{2A}^2 V_{AC}(\vec{k}_2) + \\ &c_B^2 \eta_{2B}^2 V_{BC}(\vec{k}_2) + c_B c_A \eta_{2A} \eta_{2B} (V_{BC}(\vec{k}_2) + V_{AC}(\vec{k}_2) - V_{AB}(\vec{k}_2)) + 2c_A^2 \eta_{3A}^2 V_{AC}(\vec{k}_3) + 2c_B^2 \eta_{3B}^2 V_{BC}(\vec{k}_3) + \\ &2c_A c_B \eta_{3A} \eta_{3B} (V_{BC}(\vec{k}_3) + V_{AC}(\vec{k}_3) - V_{AB}(\vec{k}_3)) + \frac{k_B T}{4} [c_A(1 + \eta_{2A} + 2\eta_{3A}) \ln(c_A(1 + \eta_{2A} + 2\eta_{3A})) + \\ &c_B(1 + \eta_{2B} + 2\eta_{3B}) \ln(c_B(1 + \eta_{2B} + 2\eta_{3B})) + (1 - c_A(1 + \eta_{2A} + 2\eta_{3A}) - c_B(1 + \eta_{2B} + 2\eta_{3B})) \\ &\ln(1 - c_A(1 + \eta_{2A} + 2\eta_{3A}) - c_B(1 + \eta_{2B} + 2\eta_{3B})) + c_A(1 + \eta_{2A} - 2\eta_{3A}) \ln(c_A(1 + \eta_{2A} - 2\eta_{3A})) + \\ &c_B(1 + \eta_{2B} - 2\eta_{3B}) \ln(c_B(1 + \eta_{2B} - 2\eta_{3B})) + (1 - c_A(1 + \eta_{2A} - 2\eta_{3A}) - c_B(1 + \eta_{2B} - 2\eta_{3B})) \\ &\ln(1 - c_A(1 + \eta_{2A} - 2\eta_{3A}) - c_B(1 + \eta_{2B} - 2\eta_{3B}))] + \frac{k_B T}{2} [c_A(1 - \eta_{2A}) \ln(c_A(1 - \eta_{2A})) + c_B(1 - \eta_{2B}) \\ &\ln(c_B(1 - \eta_{2B})) + (1 - c_A(1 - \eta_{2A}) - c_B(1 - \eta_{2B})) \ln(1 - c_A(1 - \eta_{2A}) - c_B(1 - \eta_{2B}))] \end{aligned} \quad (11)$$

where  $V_{\alpha\beta}(\mathbf{k}_3)$  is

$$V_{\alpha\beta}(\vec{k}_3) = -4 V_{\alpha\beta}^1 + 2 V_{\alpha\beta}^2 - 8 V_{\alpha\beta}^3 - 4 V_{\alpha\beta}^4 \quad (12)$$

Note that  $\mathbf{k}_2$  vector is the same as  $\mathbf{k}_1$  in a  $L_{12}$  structure.

In the disordered high-temperature phase the long-range order parameter equal zero by definition and the free energy of this phase can be written as

$$F(\text{disordered}) = \frac{1}{2}[(V_{BC}(\bar{0}) + V_{AC}(\bar{0}) - V_{AB}(\bar{0}))c_A c_B + V_{BC}(\bar{0})c_B^2 + V_{AC}(\bar{0})c_A^2] + k_B T'(c_A \ln c_A + c_B \ln c_B + (1 - c_A - c_B) \ln(1 - c_A - c_B)) \tag{13}$$

In order to calculate the free energy of each phases, the interatomic interchange energy must be estimated. We chose the same interaction parameters which were used for the computer simulation of atomic ordering in the pseudobinary Ni<sub>3</sub>Al-Ni<sub>3</sub>V system [3]. They are assumed to be: for Ni and Al interaction (mev/atom), V<sub>1</sub>=122.30, V<sub>2</sub>=6.0, V<sub>3</sub>=-16.58 and V<sub>4</sub>=-6.82; for Ni and V interaction, V<sub>1</sub>=107.2, V<sub>2</sub>=-32.0, V<sub>3</sub>=-9.6 and V<sub>4</sub>=-12.8; and for Al and V interaction, V<sub>1</sub>=40.0, V<sub>2</sub>=-30.0, V<sub>3</sub>=-80.0 and V<sub>4</sub>=-0.0. These values are closed to those derived by Caudron et al. [9] from diffusion scattering experiment and to those which were determined by Monte Carlo simulations [5]. The free energies of the ordered L<sub>12</sub> and DO<sub>22</sub> phases as a function of composition at given temperature can be evaluated by minimizing equations (6) and (11) with respect to the order parameters. Finally, the binary phase diagrams can be obtained numerically by the common tangent construction. The calculated and experimental binary phase diagrams for Ni-Al and Ni-V systems are shown in Fig. 5a and Fig.5b. It can be seen that a reasonably good fit is obtained for the phase boundaries between disordered and the mixture of disordered and ordered phases for both phase diagrams. However, for Ni-Al system the fit is as not as good as for Ni-V system. The phase boundary of the L<sub>12</sub> structure is shifted to higher concentration of Ni. In spite of this, the kinetics of atomic ordering in pseudobinary Ni<sub>3</sub>Al-Ni<sub>3</sub>V system gives a good agreement with experimental observations [4]. Therefore, we chose the same interaction energy to evaluate the ternary phase diagram.

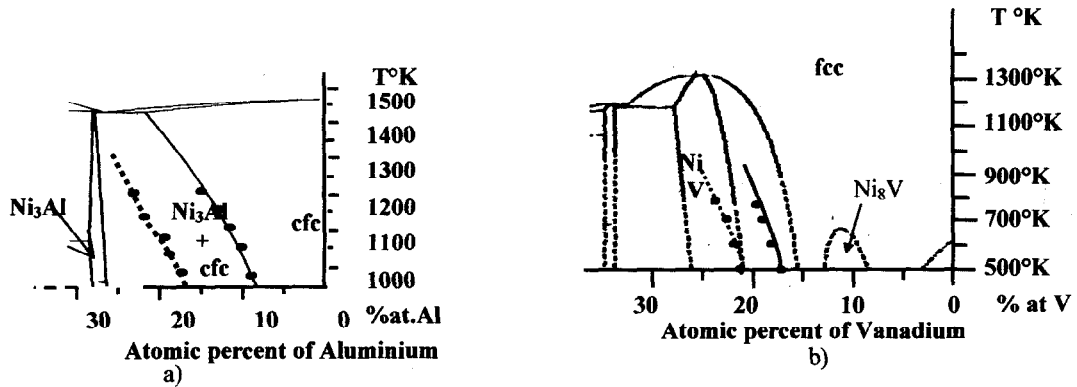


FIG.5

a) Experimental binary phase diagram for Ni-Al alloy [12], b) Experimental binary phase diagram for Ni-V alloy [12].

- corresponds to the calculated solubility limits.

**Numerical results**

To determine the equilibrium compositions of phases in the ternary systems, the tangent plane to three free energy surfaces has to be constructed. The free energy  $F(c)$  of the L<sub>12</sub> and DO<sub>22</sub> ordered phases was obtained by minimization of equations (6) and (11) with respect to their long range order parameters and the free energy of the disordered phase was calculated from equation (13). The surfaces of the free energy may be drawn on the vertical sides of a prismatic model formed by vertical free energy axes from the horizontal composition triangle. The

common tangent line, which defines the equilibrium in a binary system, is replaced by a tangent plane for ternary alloys.

Let us define the points of contact of the tangent plane with the three free energy surfaces as  $O_1, O_2$  and  $O_3$ . To construct this tangent plane we have to find the equation of a tangent plane to each surface of the free energy. The tangent plane to one surface, determined by a function  $F^i(c_A, c_B)$ , can be define as

$$A^i(c_A^i - c_{A0}^i) + B^i(c_B^i - c_{B0}^i) + (F^i(c_A, c_B) - F^i(c_{A0}^i, c_{B0}^i)) + D^i = 0 \quad (14)$$

where the coefficients A,B and D are given by

$$A^i = \frac{\partial F^i(c_A^i, c_B^i)}{\partial c_A^i} \Big|_{\substack{c_A^i=c_{A0}^i \\ c_B^i=c_{B0}^i}} \quad B^i = \frac{\partial F^i(c_A^i, c_B^i)}{\partial c_B^i} \Big|_{\substack{c_A^i=c_{A0}^i \\ c_B^i=c_{B0}^i}}$$

$$D^i = -c_{A0}^i \frac{\partial F^i(c_A^i, c_B^i)}{\partial c_A^i} \Big|_{\substack{c_A^i=c_{A0}^i \\ c_B^i=c_{B0}^i}} - c_{B0}^i \frac{\partial F^i(c_A^i, c_B^i)}{\partial c_B^i} \Big|_{\substack{c_A^i=c_{A0}^i \\ c_B^i=c_{B0}^i}} + F^i(c_{A0}^i, c_{B0}^i) \quad (15)$$

here  $c_{A0}^i$  and  $c_{B0}^i$  are the points where the plane is in contact with the free energy surface, index  $i$  labels the three phases ( $i=1,2,3$ ). To find the common tangent plane for the three free energy surfaces, which corresponds to the free energy of the  $L_{12}$ ,  $DO_{22}$  and disordered phase, the coefficients A,B and D for all three tangent planes should be equal. The conditions  $A^{\text{dis}}=A^{L_{12}}=A^{DO_{22}}$ ,  $B^{\text{dis}}=B^{L_{12}}=B^{DO_{22}}$  and  $D^{\text{dis}}=D^{L_{12}}=D^{DO_{22}}$  give the three points which determine the triangle on the isothermal section of the ternary diagram at given temperature where the three phases coexist. Tangent planes to two free energy surfaces generate tie-lines which define the equilibrium compositions of two phases. The full ternary phase diagram is generated by rotating the tangent plane over the free energy surfaces.

Experimental and calculated phase diagrams at 800°C are shown in figure 1. Table 1 gives a comparison of the experimental data derived from atom-probe analyses and the data generated by the mean field model. It is seen that the equilibrium compositions of the  $L_{12}$ ,  $DO_{22}$  and disordered phases calculated from our model are in good agreement with an experimental results obtained by 3DAP analyses.

### Discussion

The ternary NiAlV alloy is a complicated system where two ordered and one disordered phases coexist at certain temperature and composition ranges. It is difficult to study this system experimentally. In a ternary alloy microstructure, the disordered phase is localized between the different variants of the same ordered phase or between the precipitates of different phases.

Using the 3DAP technique, the local compositions of each species in the ternary  $Ni_{78.5}Al_{7.5}V_{14.5}$  alloy have been determined. Our experimental data strongly suggest that the composition of the  $L_{12}$  ordered phase is quite different from those indicated in existing phase diagrams [2]. It is shown that the composition of aluminium in the  $\gamma'$  phase is approximately the same as vanadium whereas in the published phase diagrams, the composition of aluminium is higher than vanadium. The same result is obtained by numerical calculations using the microscopic mean field model. The higher concentration of vanadium in  $\gamma'$  precipitates than that shown in the existing phase diagram can be understood by taking into account the symmetry of the  $L_{12}$  and  $DO_{22}$  superstructures. The  $L_{12}$  structure is generated by the wave vector  $k=(001)$  while the  $DO_{22}$  superstructure is formed by two wave vectors  $k=(001)$  and  $k=(1\frac{1}{2}0)$ . Previous theoretical study of the  $DO_{22}$  structure [11] have shown that the first stage of phase transformation from disordered f.c.c. phase to ordered  $DO_{22}$  structure involves ordering with the wave vector  $k=(001)$ , followed by the appearance of  $(0\frac{1}{2}1)$  wave. Therefore, a superstructure with the wave vector  $k=(001)$  provides a favourable environment for vanadium atoms. This explains the high concentration of vanadium atoms in the  $L_{12}$  precipitates. The  $DO_{22}$  superstructure does not exist in the Ni-Al system. Consequently, the aluminium concentration in  $DO_{22}$  is very small. Experimental and numerical calculations also show that the solubility limits of the disordered f.c.c. phase is also slightly different from those in the existing phase diagram. We found a higher aluminium concentration in the disordered phase than that in the existing phase diagram. Since the aluminium atoms are replaced by the vanadium in the  $L_{12}$  structure, those aluminium atoms move to the disordered matrix. Phase equilibria between  $\gamma$  and  $\gamma'$  phases in the Ni-rich portions of the NiAlX ternary systems were investigated between 800°C and 1300°C by C.C. Jia *et al* [13]. It was shown, that in the case of Ni-Al-V system, the partition coefficient

$k^{\gamma/\gamma'} = c_v^{\gamma}/c_v^{\gamma'}$  for the vanadium atoms is larger than 1, indicating higher vanadium concentration in  $\gamma$  than  $\gamma'$ . The tie-lines at 1100°C are in good agreement with the isothermal section of the existing ternary phase diagram. However, at 800°C (fig. 2) they show that the solubility limit of V(Al) in the  $\gamma'$  phase is larger (smaller) than the existing phase diagram indicates. This result shows a good agreement with our experimental data as well as numerical results. The agreement between the results from the 3DAP and numerical calculations indicated that the set of interaction parameters used in the mean-field model are reasonable in describing the thermodynamics of the NiAlV system at the temperatures of interest.

### Conclusions

The isothermal section at 800°C Ni-rich corner of the ternary phase diagram in Ni-Al-V system has been studied using three dimensional atom probe analyses and numerical calculations based on microscopic mean field approach. Both techniques showed that the solubility limits of the coexisted phases are different from those given by published phase diagrams [2]. It is found that the concentration of vanadium and aluminium are similar in the L1<sub>2</sub> ordered phase while in the existing phase diagrams the vanadium concentration is lower. In the disordered phase, we found that the aluminium concentration is slightly higher than that in the existing phase diagram. However, the solubility limits of aluminium and vanadium in the DO<sub>22</sub> ordered phases are similar to the existing phase diagram.

**Acknowledgements**—The authors wish to thank P. Caron (ONERA) for providing materials and Jean-Guy Caputo for fruitful discussions.

### References

1. Y.M. Hong, Y. Mishima and T. Suzuki, *Mat.Res.Soc.Symp.Proc.*, **133** (1989) 429.
2. F.H. Hayes, P. Rogl and E. Schmid, *Ternary Alloys*, p.8 ed. Petzow G. and Effenberg G., Weinheim: VCH, 1993
3. R. Poduri and L.Q. Chen, *Acta mater.*, **46** (1998) 1719.
4. L.A. Bendersky, F.S. Biancaniello and M.E. Williams, in *Solid-Solid Phase Transformations*, ed. Johnson W.C., Howe J.M., Laughlin D.E. and Soffa W.A. TMS, Warrendale, PA, p.899, 1994.
5. C. Pareige and D. Blavette, *Scripta Mater.*, **44** (2001) 243.
6. A.G. Khachaturyan, *Theory of Structural Transformations in Solids*, Wiley, New York, 1983.
7. M.K. Miller and G.D. Smith: *Atom Probe Microanalysis: Principles and Applications to Materials problems*, Materials Research Society, Pittsburgh, PA, 1989.
8. D. Blavette, E. Cadel and B. Deconihout, *Mat. Character.*, **44**, n1/2, (2000) 133.
9. D. Blavette, B. Deconihout, A. Bostel, J.M. Sarreau, M. Bouet and A. Menand, *Rev.Sci. Instr.*, **64** (1993) 2911, D. Blavette; A. Bostel, J.M. Sarreau, B. Deconihout and A. Menand, *Nature* **363** (1993) 432.
10. R. Caudron, M. Safati, M. Barrachin, A. Finel, F. Ducastelle and F. Solal, *J. Phys. I. France* **2** (1992) 1145.
11. D. Le Boloch, A. Finel and R. Caudron, *Phys.Rev.,B*, **62**(18) (2000) 12082.

12. M.F. Singelton, J.L. Murray, P. Nash, *Binary Alloy Phase diagrams*, eds Massalski T.B., J.L. Muray, L.H. Bennet, H. Baker, Metals Park, Ohio: American Society for Metals, 1986.
13. C.C. Jia, K. Ishida and T. Nishizawa, *Metall.Mater.Trans. A*, **25** (1994) 473.
14. B. Sundman, B. Jansson, J.-O. Anderson, *CALPHAD* **9** (1985) 153.